EVALUATION OF STATIC PRESSURE ALONG A ROUGH BOUNDARY

by

J. L. Chao and V. A. Sandborn

April 1964

CER64VAS-JLC10

EVALUATION OF STATIC PRESSURE ALONG A ROUGH BOUNDARY

by

J. L. Chao and V. A. Sandborn

SUMMARY

An experimental study of the static pressure distribution about a roughness element in a fluid boundary layer is reported. The roughness elements were uniform spheres. A definite pressure variation exists from the top to the bottom of the roughness element. The study points out that a problem exists in the definition of static pressure distribution along a rough surface. For the specific flow studied the pressure gradient along the bottom of the roughness elements is in the opposite direction to the pressure gradient along the top of the roughness elements. An integrated pressure (which corresponded to the projected area of the sphere on the surface) was found to agree with pressures measured at a location 3/4 of the way from the bottom of the sphere.

INTRODUCTION

The investigation described in this paper was originally initiated with the primary purpose of studying the shear stress on a solid rough boundary of an axisymmetry wall jet. It does not appear to be too difficult to measure the static pressure on a smooth boundary along which the fluid flows. Problems that arise are the influence of the pressure tap geometry and the hole dimensions. However, difficulties are encountered in applying the same technique on a rough boundary. What is the definition of the static pressure on a rough wall? How can one measure it?

Extensive investigations have been carried out in the past on the characteristics of the boundary layer both for the laminar and turbulent cases. However, to the authors' knowledge, there is very little information in the literature on the static pressure measurements of a rough boundary.

Einstein and El-Samni[1] have measured the hydrodynamic forces which a turbulent flow exerts on individual protrusions of a rough wall. Their primary interests were in the drag and lifting forces that the turbulent flow produces near the rough wall. Hwang and Laursen,[2] in their calibration of a Preston tube in a pipe with sandpaper fixed on the wall, measured static pressure with a thin circular disk with the pressure hole at the center. The disk was adjusted to fit on top of the sandpaper. Thus, the wall pressure was measured approximately at the top of the roughness.

This paper deals only with the pressure which the flow exerts on a particular type of roughness element. These roughness elements were lead shot. The shot elements were arranged with the maximum density

along flow path lines. The distribution of the pressure around the element was measured. The total lifting force on the element was calculated by a graphic method. This in turn permits the calculation of the average pressure which acts on the projected area of the sphere on the flat plate.

EXPERIMENTAL SET-UP AND TEST PROCEDURE

The experimental work was conducted in the Fluid Dynamics and Diffusion Laboratory, Colorado State University.

The general arrangement of the test facility is shown in figure 1. A centrifugal pump driven by a 5-HP induction motor supplied the air to a chamber through a 5-inch pipe. Two layers of screen were placed in the chamber to assist in attaining uniform mixing. The air was ejected through the sharp-edged orifice at the bottom of the chamber. The speed of the jet was controlled by a butterfly valve, and an auxiliary exhaust pipe outlet was used for making fine adjustments. The jet velocity was measured by means of a Pitot tube mounted at the center of the orifice. The jet orifice was located at a fixed position 2 feet above the top of the lead shots. The lead shots are uniform in size with the diameter of 0.18 inches. The lead shots were arranged so that a maximum density was obtained in a given area. The shots were first fixed to masking tape and then glued to the flat aluminum plate. The plate radius was 69 inches, and the part covered by the lead shots was approximately 60 inches in radius.

Five drilled balls with pressure tap located at 0^0, 30^0, 45^0, 60^0, and 90^0 respectfully, as shown in figure 2, were used for the pressure measurements. Starting at 15-3/8 inches from the center (stagnation

point), pressure taps were located at 3" intervals on the plate radially. The drilled spheres were placed at these specified positions and connecting to a pressure transducer. Atmospheric pressure was used as a reference.

The pressure difference was measured by means of a $\pm$ 0.05 psi full range strain-gage-type pressure transducer. The transducer is a differential-pressure type, consisting of a bellows and an unbounded strain gage. The output of the transducer was recorded by an X-Y plotter with the X-axis set on time base. Figure 3 shows the block diagram of the instrumentation setup and figure 4 gives the calibration of the pressure transducer.

For this particular test, the jet exit velocity was maintained at 340 fps. At each measuring station, the individual drilled balls were rotated to fixed locations in the clockwise direction. The time variation of the pressure at each location was recorded at 45^0 intervals. Therefore, as many as 33 measurements were taken at some stations. There was a slight change of barometic pressure during the data taking period. However, a check of the pressure at $\theta = 0^0$ at the start of the experiment and at $\theta = 360^0$ at the conclusion of each run showed no significant deviation.

DISCUSSION OF RESULTS

A typical recording of the time variation of pressure is shown in figure 5. The average pressure is defined by

$$\overline{P} = \lim_{T \to \infty} \frac{1}{2T} \int_{-T}^{T} p(t)dt \tag{1}$$

For practical reasons, the average time T will be finite. In the present test, all the recordings were taken over a 200-second period However, for one set of measurements three different recording times, 500 seconds, 200 seconds, 100 seconds, were taken for comparison. The mean pressure agreed within $\pm$ 0.6 % for the three-time periods.

By using spherical coordinates, as shown in figure 2, the total force on the sphere can be calculated as follows:

$$F = \int_0^{\frac{\pi}{2}} \int_0^{2\pi} p\, R^2 \,\mathrm{Sin}\, \phi \, d\theta d\phi \tag{2}$$

and in turn, this information can be used to obtain the total form drag force in the radial direction and lifting force on the sphere, i.e.,

$$D = \int_0^{\frac{\pi}{2}} \int_0^{2\pi} (p \,\mathrm{Sin}\, \phi \,\mathrm{Cos}\, \theta)\, R^2 \,\mathrm{Sin}\, \phi \, d\theta d\phi \tag{3}$$

and

$$L = \int_0^{\frac{\pi}{2}} \int_0^{2\pi} (p \,\mathrm{Cos}\, \phi)\, R^2 \,\mathrm{Sin}\, \phi \, d\theta d\phi \tag{4}$$

Figure 6 is a typical set of measured pressure distributions around the sphere. Table I lists the complete set of measurements made for the present study.

Knowing the total drag force in the radial direction and total uplift force acted on a sphere, the shear stress and the average pressure on the projected area of the sphere was then calculated. The shear stress and pressure variation along the radial direction thus obtained are shown in figures 7 and 8 respectfully. These values are also listed in Table II.

In figure 9, the pressure which was measured at the top, bottom and $y = 0.75d$ of the sphere are presented for comparison.

By physical reasoning, one can see that the flow is working its way against an increasing pressure, or in other words, it is flowing against an adverse pressure gradient. However, the pressure measured at the bottom of the sphere, or along the plate top, shows a favorable pressure gradient, which contradicts the expected condition. This suggests that little confidence can be placed in the conventional technique of evaluating the static pressure measurement at the lower surface of a rough wall.

The Karman-Prandtl equation for the average velocity distribution in turbulent flow near rough boundaries is written as

$$\frac{u}{u_*} = 5.75 \log_{10} \frac{y - y_o}{K_s} + C \qquad (5)$$

In applying this equation, one has to shift the datum plane where $y = y_o$ between the top and bottom of the roughness element, in order to fit the logarithmic friction law. In many cases, [1], [3], [4] it has been found that this so called datum plane falls between approximately 0.7 to 0.8 of the height of the roughness element. From the present study, it is interesting to note, figure 9, that the pressure measured at $y = 0.75d$ (or $\phi = 60^0$, $\theta = 180^0$) agrees quite well with the average

pressure calculations. The similarity of the average pressure height to that shift in height required to fit the log velocity distribution is quite striking.

Figure 10, shows the static pressure gradient along the radial direction. If the measurements taken at $\frac{y}{d} = 0.75$ were considered as correct, the error would be unacceptable (150 %) if one used the measurements at the top of the sphere. The important point to be made from figure 10 is that a "static" pressure variation exists over a roughness element. Therefore, one measurement of pressure either at the bottom, middle or top of the element is not sufficient to define the "static" pressure for a rough surface. Large static pressure gradients are known to exist near the surface of even smooth flat plate turbulent boundary layers[5], so the presence of a pressure gradient within the roughness layer should come as no surprise.

CONCLUDING REMARKS

In the course of experimental tests in fluid flow, it has been always a rule that the flow should be disturbed as little as possible. But, on the other hand, one should also take into account all of the elements which are creating the phenomena studied. In the present investigation, attempts were made to fulfill this requirements. Issue is not taken with the applicability of this method for the static pressure measurement on any arbitrary roughness, but to emphasize this would be one way to approach the determination of the static pressure on rough boundaries. Of course, the influence of hole geometry and dimensions on the static pressure measurements, which are also present on the smooth boundary, remains a possible source of error.

Based on the experimental results, one can conclude:

First, measurement of the pressure at top or bottom of a roughness elements certainly is not a unique way to determine the static pressure gradient along the flow. Second, if the pressure which acts on the projected area of the roughness element is considered to be the wall pressure, then, in this particular flow, the pressure measured at $\frac{y}{d} = 0.75$ at the downstream face of the sphere agrees very well with the average value.

The measurement of static pressure along a rough boundary in a fluid flow is by no means well defined. More extensive research is certainly needed before we can have a better understanding of the mechanism. It still remains to be shown whether or not the projected area pressure is of value in theoretical evaluations.

REFERENCES

1. Einstein, H. A., and El Samni, A.: Hydrodynamic Forces on a Rough Wall. Review of Modern Physics, Vol. 11, No. 3, July 1949.

2. Hwang, L. S., and Laursen, E. M.: Shear Measurement Technique for Rough Surfaces. Journal of Hydraulic Division, ASCE, March 1963.

3. Perry, A. E., and Joubert, D. N.: Rough Wall Boundary Layers in Adverse Pressure Gradients. Journal of Fluid Mechanics, Vol. 17, Part 2, October 1963.

4. Moore, W. F.: An Experimental Investigation of the Boundary Layer Development Along a Rough Surface. Ph.D. Dissertation, State University of Iowa, 1951.

5. Sandborn, V. A., and Slogar, R. J.: Study of the Momentum Distribution of Turbulent Boundary Layers in Adverse Pressure Gradients. NACA TN 3264, 1955.

TABLE I MEASURED DATA

ϕ	$rd\phi$	θ	$r \sin \phi d\theta$	$\Delta p \times 10^{-4}$ -- psi (Atm. pressure used as ref. pressure)							
degree	in	degree	in	R = $15\frac{3}{8}$"	$18\frac{3}{8}$"	$21\frac{3}{8}$"	$24\frac{3}{8}$"	$27\frac{3}{8}$"	$30\frac{3}{8}$"	$33\frac{3}{8}$"	$36\frac{3}{8}$"
0	--	--	--	-9.75	-5.30	--	-2.74	--	-1.43	--	-0.707
30	0.0472	0	0.000	+19.0	+11.75	--	+6.16	--	+3.63	--	+1.495
		45	0.035	+ 5.15	+ 4.45	--	+1.73	--	+1.057	--	+0.346
		90	0.071	-1.43	- 3.08	--	-1.48	--	-1.188	--	-0.261
		135	0.106	-7.30	- 3.94	--	-2.19	--	-1.20	--	-1.04
		180	0.141	-7.63	- 3.73	--	-2.03	--	-0.758	--	-0.788
		225	0.176	-8.72	--	--	--	--	--	--	--
		270	0.212	-7.58	- 4.26	--	-1.04	--	--	--	--
		315	0.248	+ 5.15	--	--	--	--	--	--	--
		360	0.288	+23.0	+11.25	--	+6.82	--	+3.27	--	+1.81
45	0.0706	0	0.000	+18.8	+11.26	--	+5.84	--	+1.98	--	+1.11
		45	0.050	+ 9.95	+ 3.25	--	+1.39	--	+1.10	--	+0.387
		90	0.100	- 3.33	- 1.56	--	-0.80	--	-0.75	--	-0.75
		135	0.150	- 6.65	- 2.47	--	-1.10	--	-0.85	--	-0.39
		180	0.200	- 4.77	- 2.86	--	-1.05	--	-0.901	--	-0.36
		225	0.250	- 5.77	--	--	--	--	--	--	--
		270	0.300	- 3.38	- 2.04	--	-1.42	--	--	--	--
		315	0.350	+ 8.40	--	--	--	--	--	--	--
		360	0.400	+21.0	+11.7	--	+5.00	--	+1.98	--	+0.901

TABLE I MEASURED DATA (cont'd)

ϕ	$rd\varphi$	θ	$r \sin \phi d\theta$	$\Delta p \times 10^{-4}$ -- psi (Atmo. pressure used as ref. pressure)							
degree	in	degree	in	R = $15\frac{3}{8}$"	$18\frac{3}{8}$"	$21\frac{3}{8}$"	$24\frac{3}{8}$"	$27\frac{3}{8}$"	$30\frac{3}{8}$"	$33\frac{3}{8}$"	$36\frac{3}{8}$"
60	0.0942	0	0.000	+21.8	+11.6	--	+4.08	--	+1.54	--	+0.67
		45	0.061	+ 4.68	+ 7.17	--	+3.53	--	+0.80	--	+0.261
		90	0.122	+ 0.55	- 3.47	--	-1.60	--	-0.307	--	-0.526
		135	0.184	- 3.58	- 4.04	--	-2.08	--	-0.775	--	-0.185
		180	0.245	- 3.60	- 1.62	--	-0.83	--	-0.354	--	-0.337
		225	0.305	- 3.22	--	--	--	--	--	--	--
		270	0.375	- 0.62	--	--	-1.48	--	+0.78	--	--
		315	0.429	+ 7.85	--	--	--	--	--	--	--
		360	0.490	+23.8	+12.0	--	+3.88	--	+1.39	--	+0.67
90	0.141	0	0.000	+ 5.03	+ 1.67	--	+1.27	--	+0.59	--	+0.252
		45	0.0705	+ 2.13	+ 1.32	--	+1.06	--	0	--	+0.783
		90	0.141	+ 0.915	+ 1.28	--	+0.84	--	+0.169	--	-0.333
		135	0.212	+ 0.81	+ 1.30	--	+0.42	--	+0.0072	--	-0.257
		180	0.283	+ 0.373	+ 0.38	--	+0.21	--	+0.0156	--	-0.286
		225	0.353	+ 0.375	--	--	--	--	--	--	--
		270	0.424	+ 1.35	+ 1.07	--	--	--	--	--	--
		315	0.495	+ 3.00	--	--	--	--	--	--	--
		360	0.565	+ 4.84	+ 2.04	--	--	--	+0.442	--	--
Bot. of Sphere				+ 4.22	+ 1.48	+0.844	+0.633	+0.422	+0.211	0.0	0.0

TABLE II AVERAGE PRESSURE AND SHEAR STRESS

R	L	D	p_w	τ_w
in	lbs	lbs	psi	psi
$15\frac{3}{8}$	-8.32×10^{-6}	1.56×10^{-5}	-3.28×10^{-4}	6.12×10^{-4}
$18\frac{3}{8}$	-4.80×10^{-6}	1.15×10^{-5}	-0.944×10^{-4}	4.54×10^{-4}
$24\frac{3}{8}$	-1.41×10^{-6}	0.557×10^{-5}	-0.277×10^{-4}	2.19×10^{-4}
$30\frac{3}{8}$	-1.196×10^{-6}	0.220×10^{-5}	-0.235×10^{-4}	0.872×10^{-4}
$36\frac{3}{8}$	-1.183×10^{-6}	0.134×10^{-5}	-0.233×10^{-4}	0.527×10^{-4}

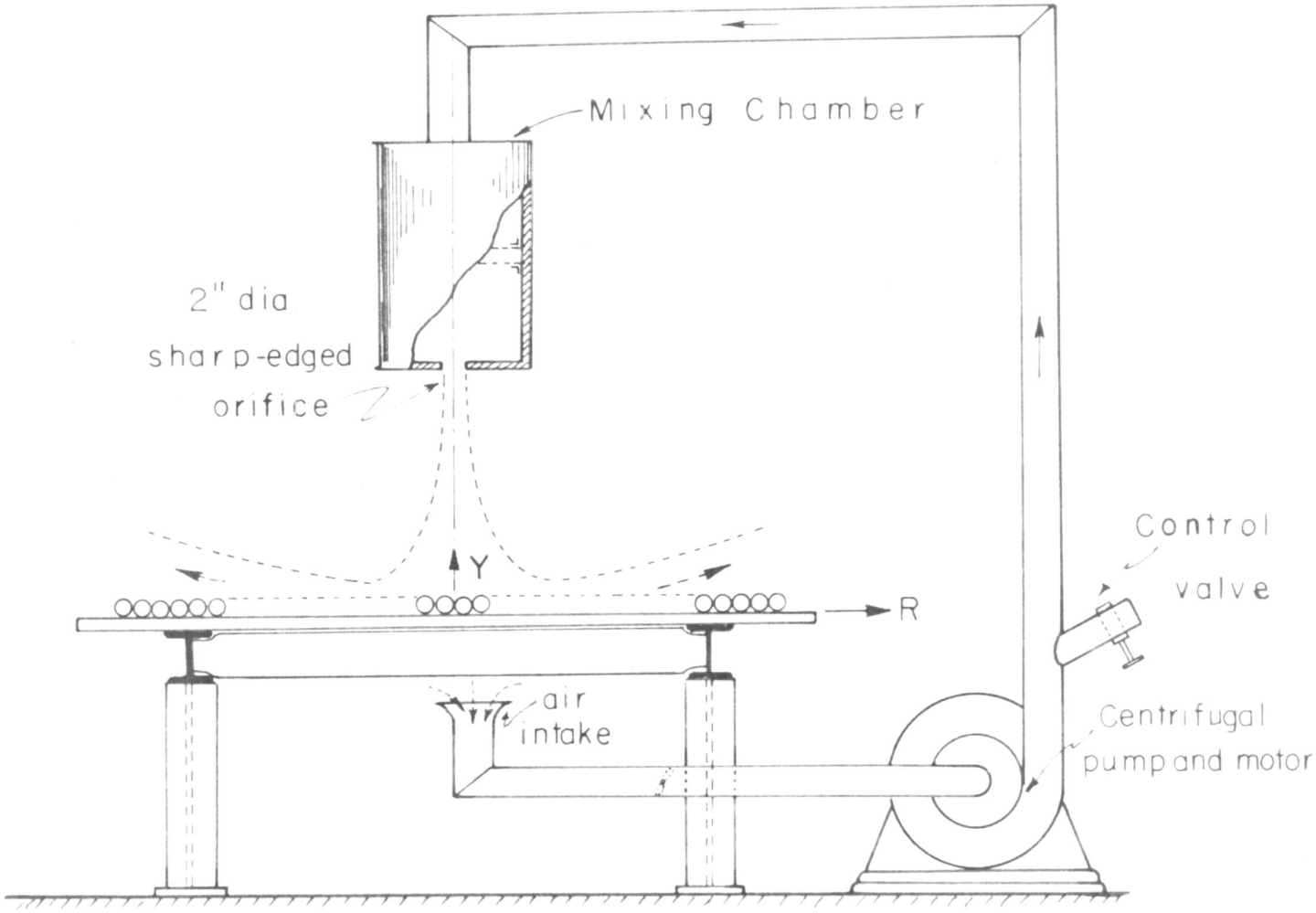

Fig. 1

General Setup of Experiment

(Not to scale)

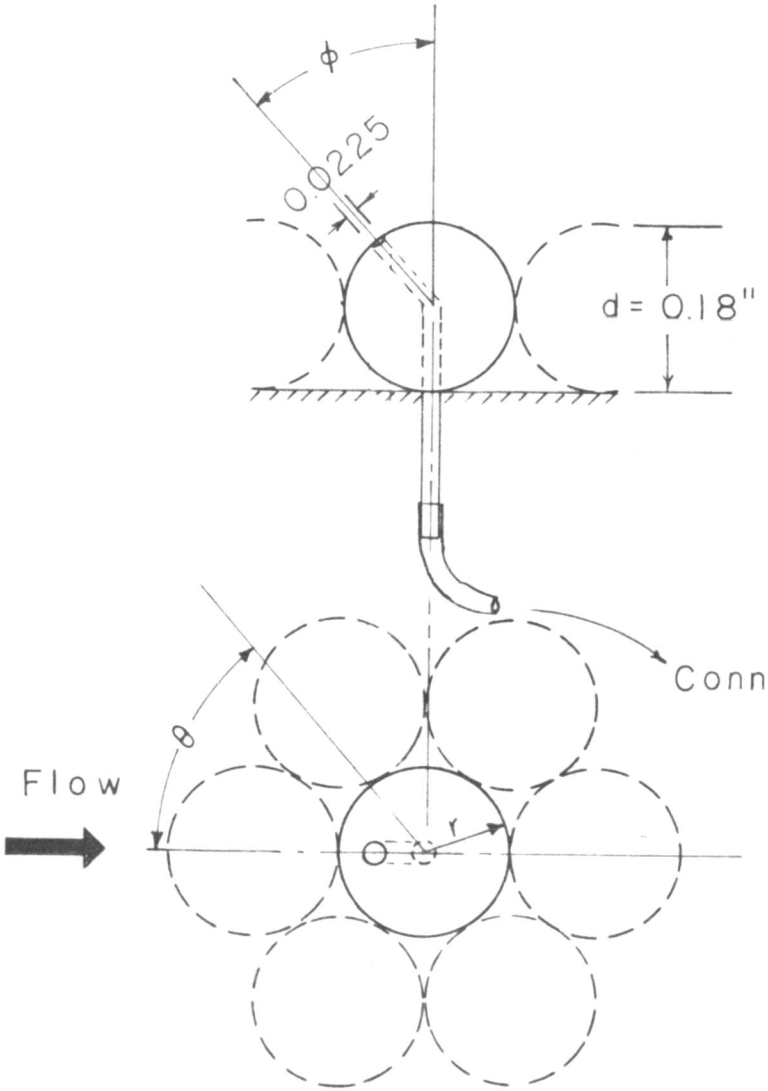

sphere No.	φ	r
1	0°	0.09 in.
2	30°	0.09 in.
3	45°	0.09 in.
4	60°	0.09 in.
5	90°	0.09 in.

Fig. 2

Detail of Balls used for Pressure Measurements

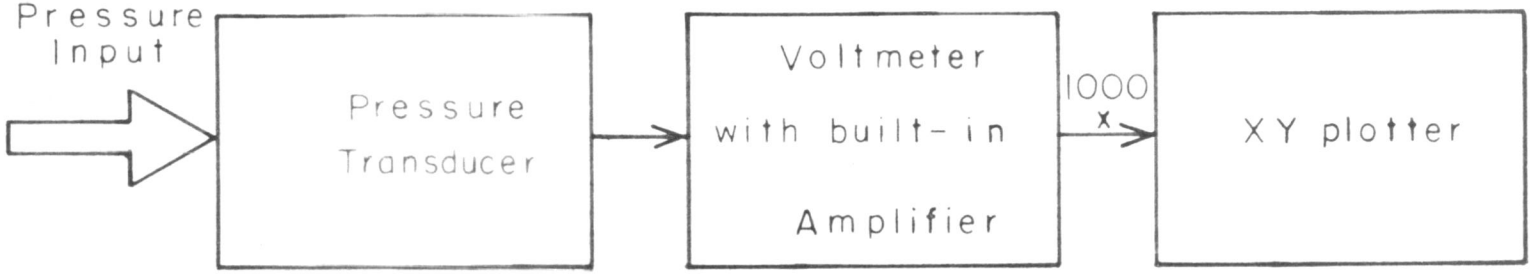

Fig. 3
Instrumentation
Setup

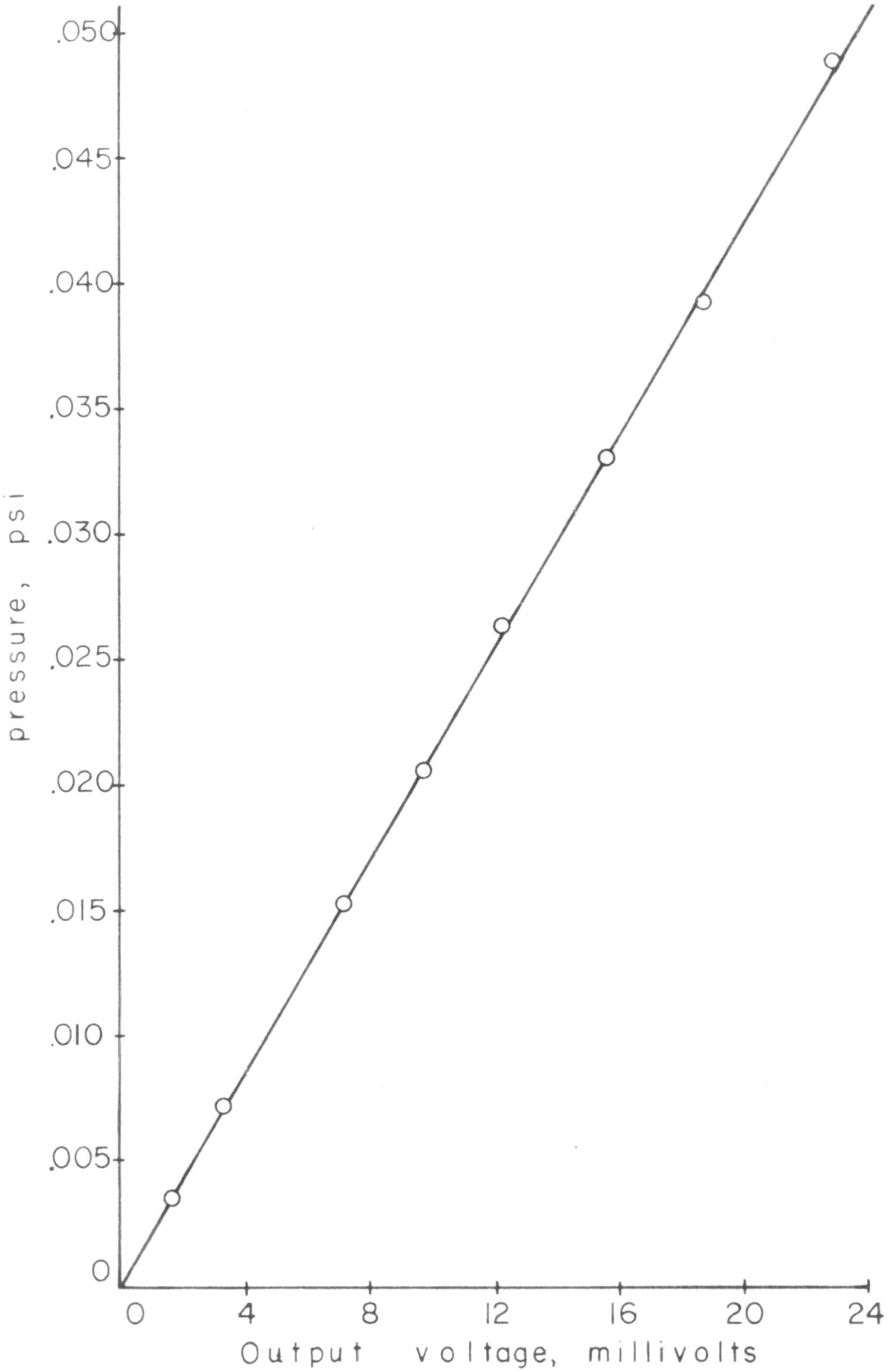

Fig.4 Calibration of the ± 0.05 psi pressure transducer

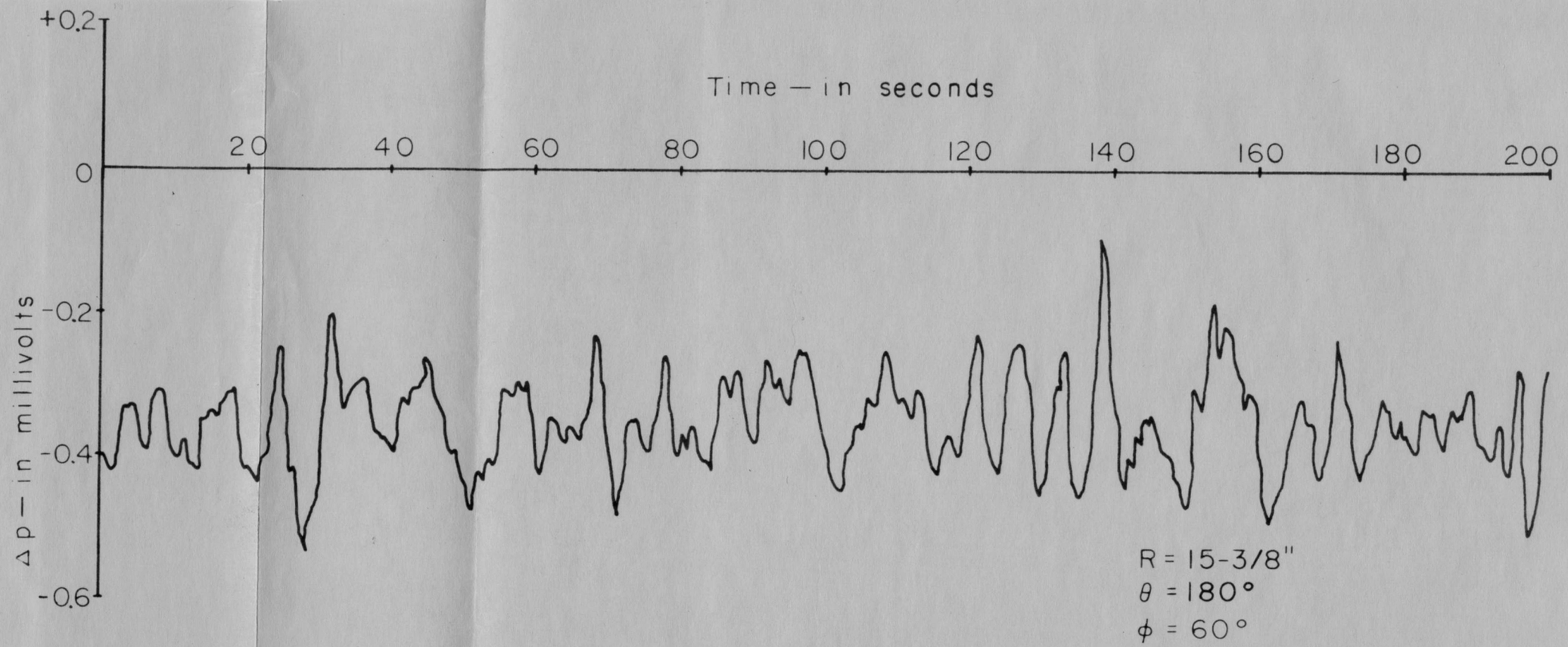

Fig 5

Typical Time Variation of Pressure

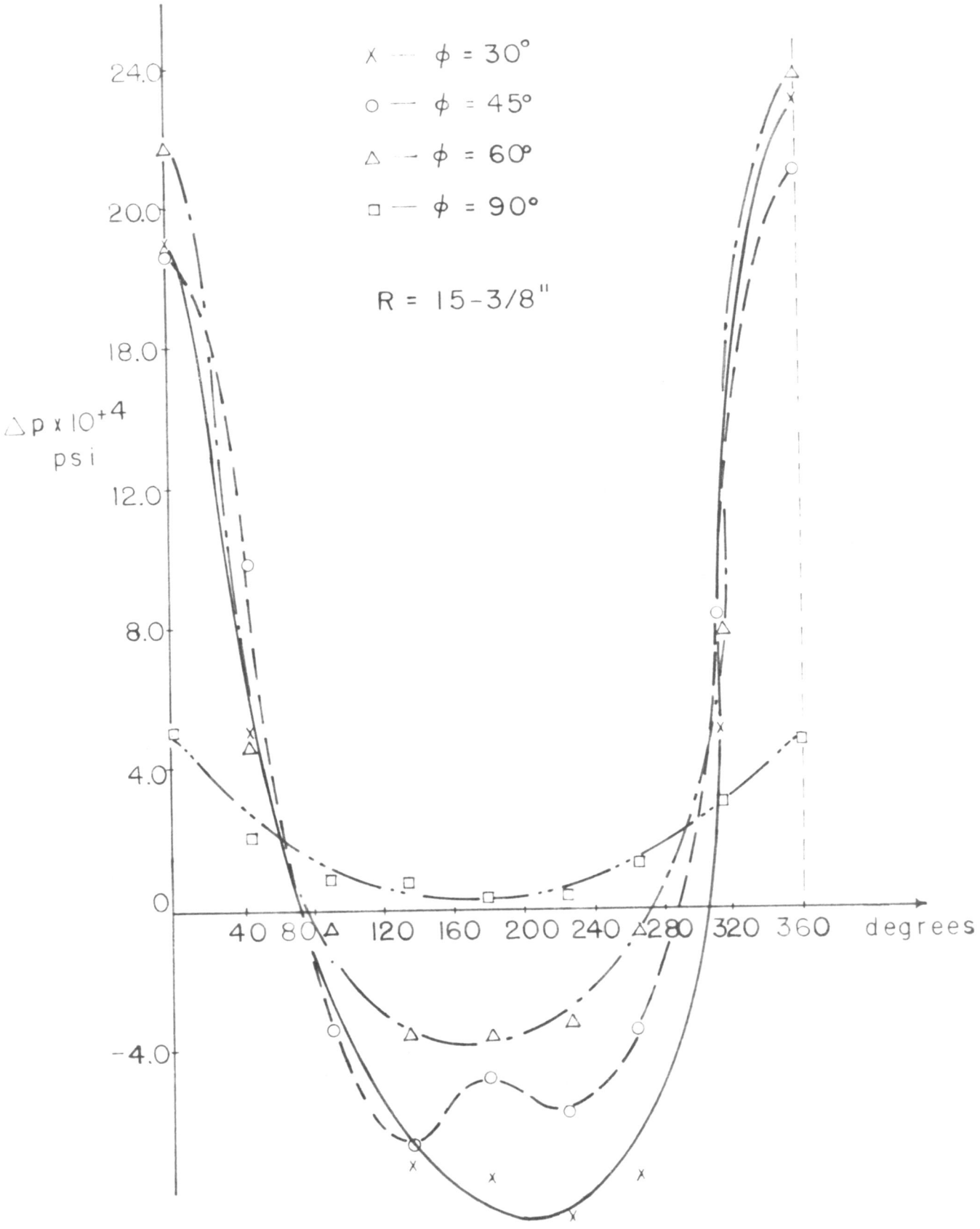

Fig.6 Pressure Distribution around the Sphere

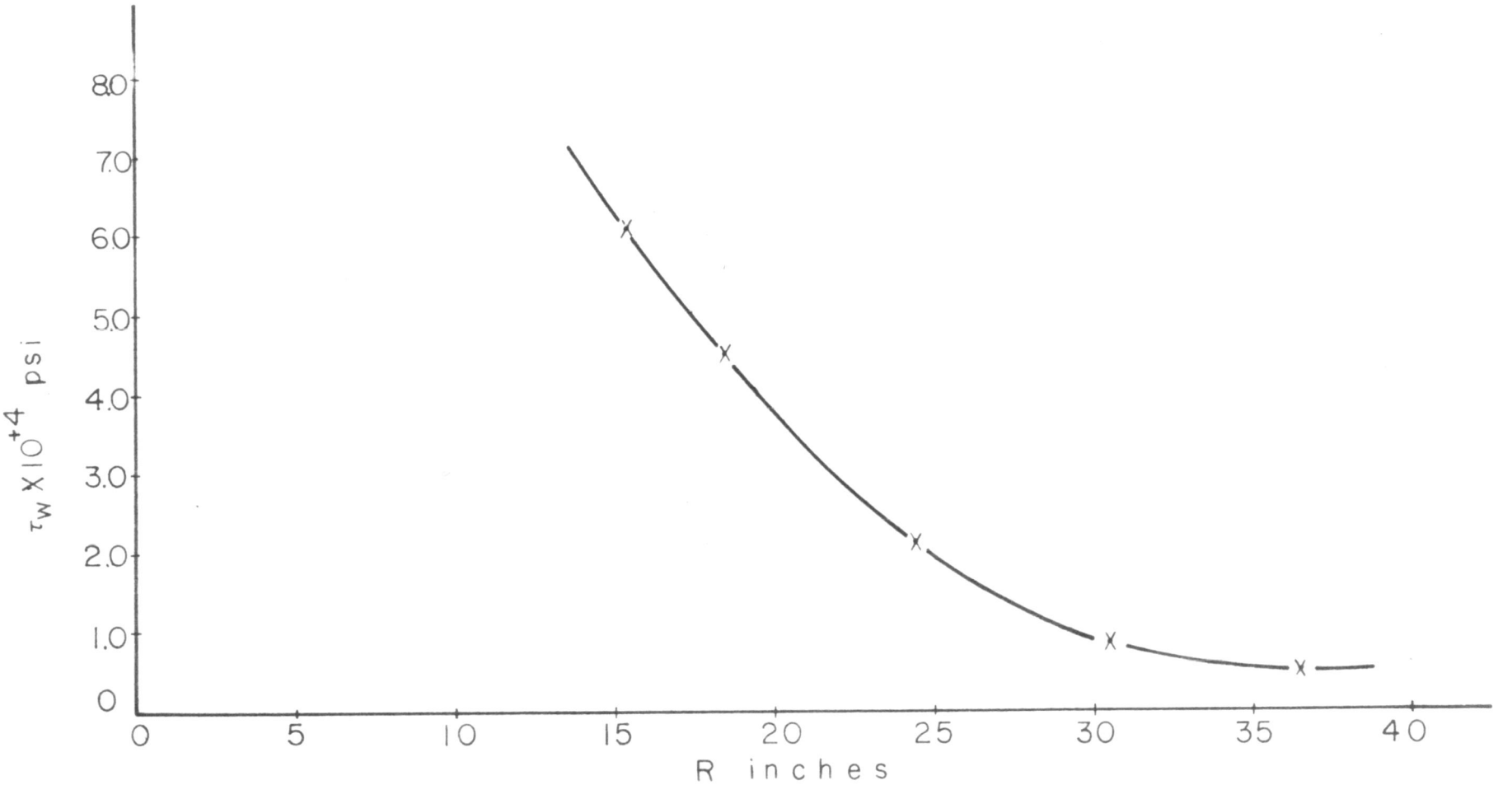

Fig. 7

Calculated wall shear stress along the radial direction

note: Atmospheric pressure used as reference

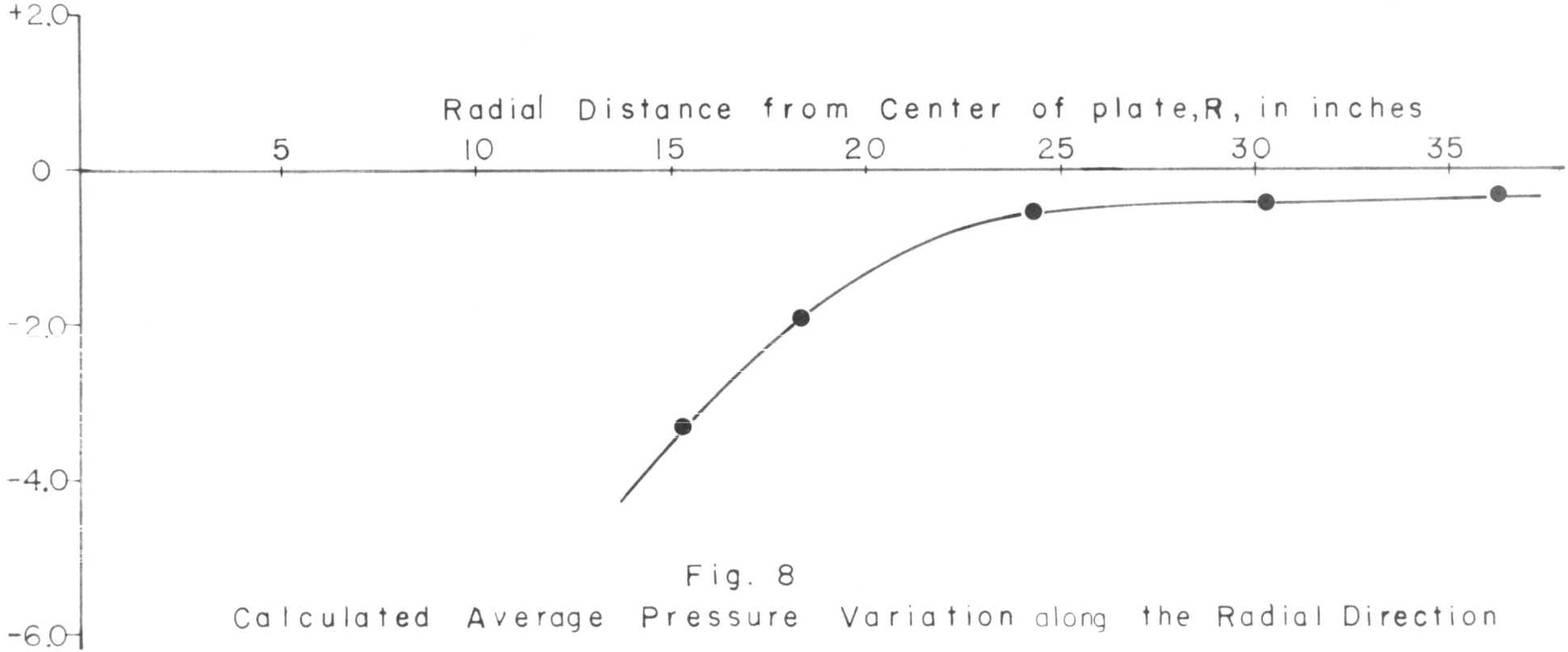

Fig. 8
Calculated Average Pressure Variation along the Radial Direction

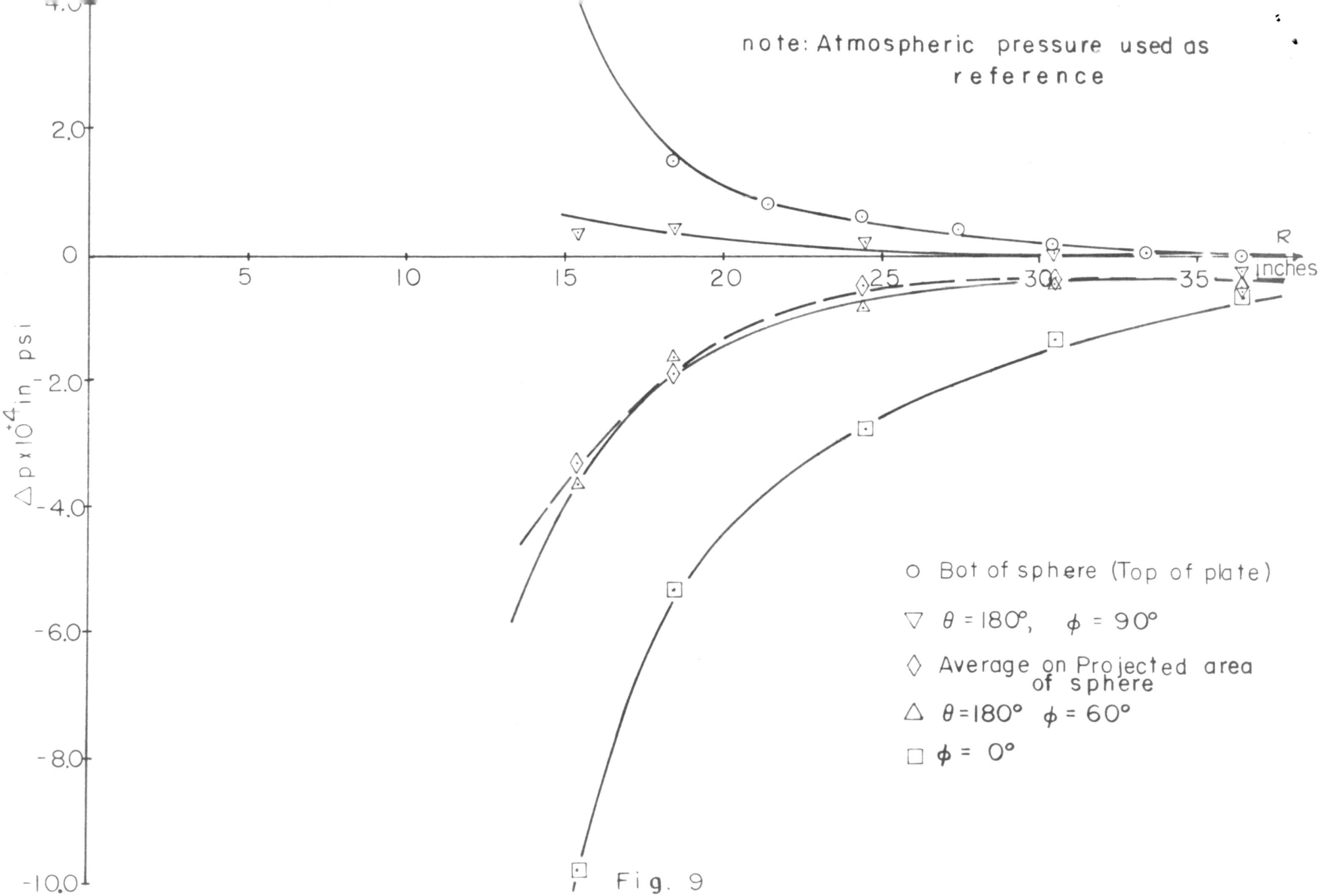

Fig. 9

Comparison of Pressure Variation in the Radial Direction

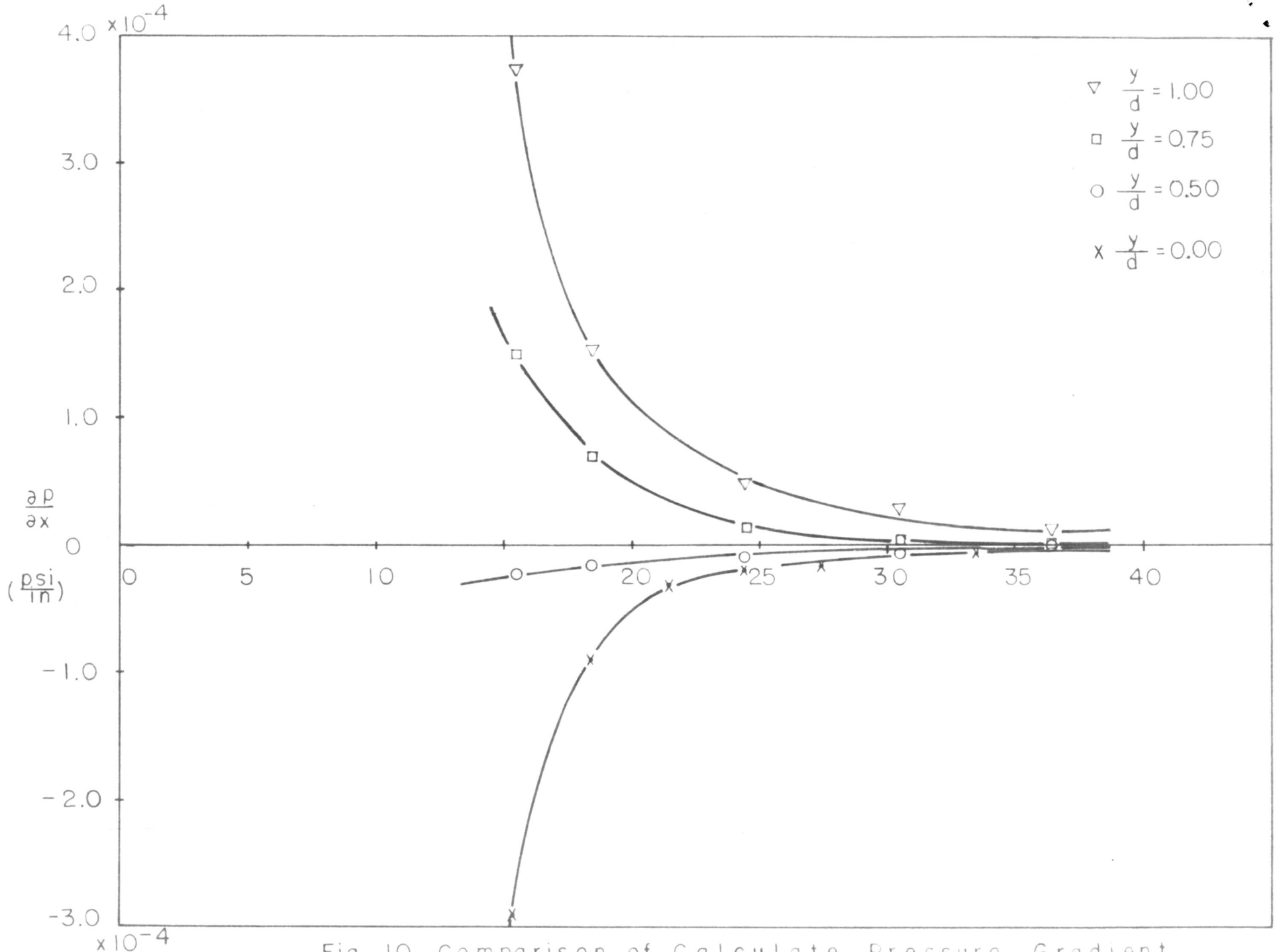

Fig. 10 Comparison of Calculate Pressure Gradient